The Two-Pathway Model of the Biological Catch-Bond as a Limit of the Allosteric Model

Yuriy V. Pereverzev,[†] Eugenia Prezhdo,[†‡] and Evgeni V. Sokurenko[‡*]
[†]Department of Chemistry, University of Rochester, Rochester, New York; and [‡]Department of Microbiology, University of Washington, Seattle, Washington

ABSTRACT Catch-binding is a counterintuitive phenomenon in which the lifetime of a receptor/ligand bond increases when a force is applied to break the bond. Several mechanisms have been proposed to rationalize catch-binding. In the two-pathway model, the force drives the system away from its native dissociation pathway into an alternative pathway involving a higher energy barrier. Here, we analyze an allosteric model suggesting that a force applied to the complex alters the distribution of receptor conformations, and as a result, induces changes in the ligand-binding site. The model assumes explicitly that the allosteric transitions govern the properties of the ligand site. We demonstrate that the dynamics of the ligand is described by two relaxation times, one of which arises from the allosteric site. Therefore, we argue that one can characterize the allosteric transitions by studying the receptor/ligand binding. We show that the allosteric description reduces to the two-pathway model in the limit when the allosteric transitions are faster than the bond dissociation. The formal results are illustrated with two systems, P-selectin/PSGL-1 and FimH/mannose, subjected to both constant and time-dependent forces. The report advances our understanding of catch-binding by combining alternative physical models into a unified description and makes the problem more tractable for the bond mechanics community.

INTRODUCTION

Recent years have witnessed increased interest in the biophysics of receptor/ligand complexes, such as FimH/mannose, P,L,E-selectin/PSGL-1, and others (1–7), showing an unusual dependence of the complex lifetime on the magnitude of an external force applied to rupture the bond. For a constant force, the lifetime of the complex grows initially with increasing force magnitude, contradicting the common expectation. Only at a certain force threshold does the lifetime reaches a maximum and start decreasing. In the jump/ramp experiments when the force grows linearly with time, such receptor/ligand complexes exhibit an anomaly in the probability distribution for the rupture force. Namely, for sufficiently slow force ramping, there exists an unusually high probability of bond rupture at small forces.

Several theoretical models (8–21) have been proposed to explain the observed phenomenon. This article focuses on the two-pathway (12) and allosteric (19) models that provide seemingly different physical interpretations of the catch-binding phenomenon. This article establishes a direct connection between the two descriptions. Fig. 1 illustrates, in schematic fashion, creation of the receptor/ligand complex and its dissociation that is coupled to the force-induced allosteric transition between the two conformations of the receptor protein. The diagram also illustrates how the two protein conformations lead to the catch- and slip-pathways of the two-pathway model. Fig. 2 shows the corresponding free energy profiles for the conformational change in the receptor protein and for the receptor/ligand interaction. It should be emphasized that the two-state potential for the allosteric site is separated from the single-state potential describing the receptor/ligand binding, as clearly seen in Fig. 2 *a*. This creates important distinctions between the current allosteric model and other multiparameter models (10,11,13).

The two-pathway model (12) provides the simplest mathematical description of the catch-slip transition, leading to many useful analytical results and predictions (22–25). It assumes that the free energy profile for the receptor/ligand interaction (Fig. 2 *b*) contains one minimum *l*, describing the bound state, and two alternative pathways of escape from the minimum, describing the catch and slip mechanisms of the bond dissociation. In this model, the dependence of the bond dissociation rate constant $k(f)$ on the applied force f has the simple expression:

$$k(f) = k_s^0 \exp\left[\frac{x_s f}{T}\right] + k_c^0 \exp\left[\frac{-x_c f}{T}\right]. \qquad (1)$$

Here, k_s^0 and k_c^0 are the rate coefficients for the bond dissociation via the slip (s) and catch (c) pathways in the absence of force. For brevity, we use T in Eq. 1 and below to denote the product of the Kelvin temperature and the Boltzmann constant k_B. The force dependence of the Kramer's rate coefficient in Eq. 1 is introduced according to Bell (26). The parameters x_s and x_c are the distances from the minimum to the corresponding maxima of the potential (Fig. 2 *b*). According to Eq. 1, an increasing force accelerates the bond dissociation via the slip pathway and decelerates the dissociation via the catch pathway. Within a certain

Submitted July 7, 2011, and accepted for publication August 11, 2011.

*Correspondence: evs@u.washington.edu or evgeni.sokurenko@gmail.com

Editor: R. Astumian.

0006-3495/11/10/2026/11 $2.00

doi: 10.1016/j.bpj.2011.09.005

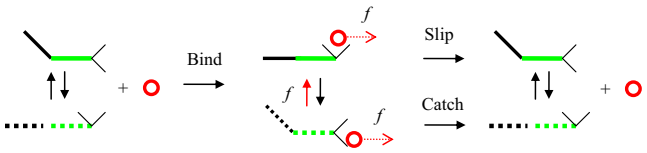

FIGURE 1 Binding and dissociation of a receptor/ligand catch-bond complex. The diagram is based most directly on the FimH/mannose system (27,44); however, it also represents other catch-bonds. The two-domain fragment of the receptor protein, composed of the pilin (*black*) and lectin (*green*) domains, exists in either bent or extended state. (*Solid lines*) More stable conformation; (*dashes*) less stable conformation. The bent state is more favorable in the free receptor. Binding to mannose (*circle*) shifts the conformational equilibrium toward the extended state. The interaction between lectin's binding site (*angle* made of *two thin black lines*) and mannose is stronger for the extended state (*angle* holding the *circle*) than the bent state (*angle* releasing the *circle*). The applied force (*red arrows*) lowers the bond dissociation barrier and favors the extended conformation. The control of the receptor conformation by force, combined with the correlation between the receptor conformation and the receptor/ligand binding strength, forms the basis for the allosteric model (19); see also Fig. 2 *a*. The bond dissociations via the bent and extended channels represent the catch- and slip-pathways in the two-pathway model (12); see also Fig. 2 *b*.

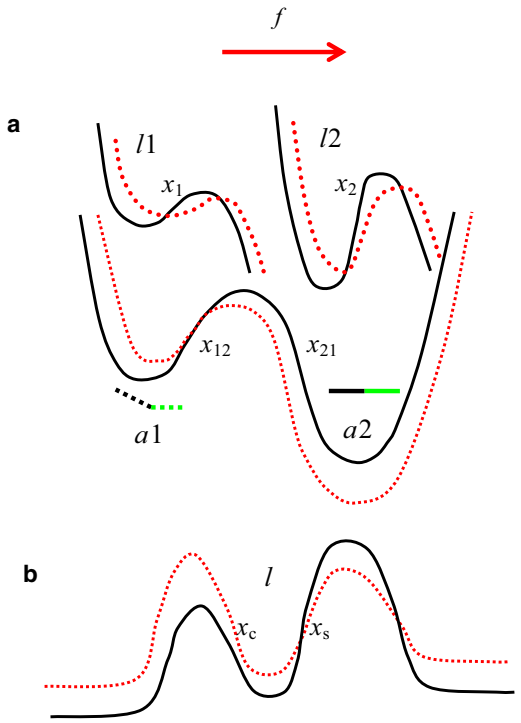

FIGURE 2 Energy profiles in the bound receptor/ligand complex for (*a*) allosteric (19) and (*b*) two-pathway (12) models of catch-binding. Minima *a*1 and *a*2 in panel *a* describe the bent and extended states of the two-domain receptor fragment, in accordance with the central part of Fig. 1. States *a*1 and *a*2 of the receptor allosteric fragment correlate with the free energy profiles *l*1 and *l*2 characterizing the ligand binding site. For a certain relationship between the model parameters, the allosteric model of panel *a* transforms into the two-pathway model of panel *b*, in which the ligand escapes from the binding site *l* via either the catch-barrier (*left*) or the slip-barrier (*right*). Application of the force (*vector arrow*) modifies the energy profiles for the allosteric and ligand interactions in panels *a* and *b* (from *solid* to *dashed curves*). All barriers are characterized by their widths *x*, as labeled in the figure. The barrier width is defined as the distance from the minimum to the maximum.

range of the model parameters (12), the competition between the two dissociation pathways leads to the catch-slip transition in the bond lifetime as a function of force.

The analysis of the catch-slip transition using the two-pathway model shows (25) that the depth of the free energy minimum describing the bound state of the receptor/ligand complex grows with force within a certain range of forces. Approaching the catch-slip phenomenon from this point of view, the concept of bond deformation was introduced in Pereverzev and Prezhdo (16). According to the deformation model, the receptor/ligand interaction strengthens as a result of a force-induced conformational change in the protein system.

The mathematical simplicity of the two-pathway model of the catch-slip transition, shown by Eq. 1, has led to a number of useful analytical results (12,22–25). At the same time, its direct physical interpretation requires understanding of the two distinct bond dissociation pathways, which are not trivial to establish for a given biological bond. This article shows that the mathematical form of the two-pathway model can be achieved within an alternative physical interpretation of catch-binding that is based on the concept of force-induced allostery (13,19,27) (see Figs. 1 and 2). The allosteric view on the two-pathway model of catch-binding provides a specific prescription to the catch and slip mechanisms of bond dissociation.

Proteins and other biological molecules are flexible objects that exhibit an ensemble of conformations at ambient temperatures. The ensemble perspective on protein properties is being actively explored by the biophysical community (28–41). In thermodynamics equilibrium, each conformation is present with some probability, whose value depends on external parameters, e.g., temperature. Local interactions, including receptor/ligand binding and external forces, can also have a profound effect on the ensemble distribution. Often, the overall conformation of the receptor protein is governed by the state of a local site, known as the allosteric site. Transitions of the allosteric site between different states propagate throughout the protein, changing its global conformation. During allosteric regulation an effector, such as a ligand or a pulling force, acting on the allosteric site in one part of a protein, induces changes in another, distant part of the protein, known as the active site.

After binding to the active site of the protein, the ligand moves in the potential, the structure of which is changing when the protein passes from one state to another. Allosteric regulation modifies the distribution of the binding potentials, and thereby affects the receptor/ligand binding. In turn, the receptor/ligand binding can shift the thermodynamic distribution of protein conformations relative to that for the free protein. The change in the ensemble of protein conformation affecting the receptor/ligand binding can

occur via allosteric regulation induced not only by another protein (42,43), but also by force applied to the allosteric site (13,43,44).

Frequently, a protein fragment composed of two domains (Fig. 1) transduces allosteric regulation. Application of an external force changes the two-domain structure, which for simplicity can be characterized by the angle between the domains. The allosteric fragment of the FimH/mannose complex involves the lectin and pilin domains (44). The domains in the P-selectin/PSGL-1 complex are lectin and EGF (43). Following Pereverzev et al. (19), we will assume that the full distribution of the interdomain angles can be represented sufficiently by two angles describing bent and extended protein conformations (Figs. 1 and 2 *a*).

The article is constructed as follows. In the next section we derive the connection between the allosteric and two-pathway model. Next, we illustrate the derived mapping with the P-selectin/PSGL-1 and FimH/mannose bonds, including both constant force and jump/ramp experiments. Then, we analyze in detail the dynamics of the ligand subjected to a constant pulling force. We show that such analysis of the ligand dynamics can be used to extract information about the properties of the allosteric site, and to establish more rigorously the relationships between the rate coefficients needed for the transition from the allosteric to the two-pathway model. We conclude by discussing how the established connection can be used to unify the various models developed for the description of the catch-slip transition and to facilitate the analysis of the experimental data.

REVIEW OF THE ALLOSTERIC MODEL

The dissociation of the receptor/ligand complex is described using three probabilities $P_1(t, f)$, $P_2(t, f)$, and $P(t, f)$ that depend on both time and force. $P_1(t, f)$ and $P_2(t, f)$ are the probabilities to find the allosteric site in the bound complex in states $a1$ and $a2$ (Fig. 2 *a*) at time t for the complex subjected to force f. States $a1$ and $a2$ of the allosteric site in Fig. 2 *a* correspond to the bent and extended conformations of the receptor protein provided that the ligand is bound to the receptor. $P(t,f)$ is the probability to find the ligand bound to the receptor at time t for force f. This approach differs in an important way from the models of Evans et al. (10), Barsegov and Thirumalai (11), and Thomas et al. (13), where the system is described, but using only two probabilities corresponding to two states of the whole receptor/ligand system. Evans et al. (10), Barsegov and Thirumalai (11), and Thomas et al. (13) do not make an explicit distinction between the probabilities in describing the allosteric and binding sites, and the sum of $P_1(t, f)$ and $P_2(t, f)$ in these models decreases to zero at long times. In contrast, in our model,

$$P_1(t,f) + P_2(t,f) = 1 \tag{2}$$

at all times. The evolution of the probabilities $P_1(t, f)$ and $P_2(t, f)$ is given by (19,45)

$$\begin{aligned} \frac{dP_1(t,f)}{dt} &= -k_{12}(f)P_1(t,f) + k_{21}(f)P_2(t,f), \\ \frac{dP_2(t,f)}{dt} &= -k_{21}(f)P_2(t,f) + k_{12}(f)P_1(t,f), \end{aligned} \tag{3}$$

where $k_{12}(f)$ and $k_{21}(f)$ are the rate constants for transitions from state $a1$ to state $a2$ and back. The force dependence of these coefficients is introduced using the Bell approximation (26,46),

$$k_{12}(f) = k_{12}^0 \exp\left(\frac{x_{12} f}{T}\right),$$

$$k_{21}(f) = k_{21}^0 \exp\left(\frac{-x_{21} f}{T}\right),$$

where k_{12}^0 and k_{21}^0 are the rate constants in the absence of force, and x_{12} and x_{21} are the distances from the first and second minima, respectively, to the top of the barrier (Fig. 2 *a*). Note the difference in the signs in the two exponents. The signs depend on the direction of the applied force and represent the fact that the force promotes transitions from $a1$ to $a2$ and obstructs transitions from $a2$ to $a1$. A time-dependent force will be denoted by the explicit notation $f(t)$. In accordance with Eqs. 2 and 3, the receptor fluctuates only between two states (Fig. 2 *a*) and in contrast to the assumptions made in Evans et al. (10), Barsegov and Thirumalai (11), and Thomas et al. (13), there exist no bond dissociation pathways out of this two-state potential.

In the case of the P-selectin/PSGL-1 and FimH/mannose systems considered in detail below, the allosteric fragments include two protein domains that move with respect to each other. Then, states $a1$ and $a2$ of the allosteric model correspond to the bent and extended conformations of the two-domain fragment. The force applied to the ends of the fragment stretches the protein, promoting the transition from the bent to the extended state and obstructing the reverse process (Figs. 1 and 2 *a*).

It is logical to associate each allosteric state of the receptor protein with a different state of the active site (Fig. 2 *a*). Each state of the allosteric sites $a1$ and $a2$, or in other words, each conformation of the receptor protein, creates its own potential for interaction with the ligands $l1$ and $l2$. According to our assumption about the governing role of the allosteric site, the ligand interacting with the receptor moves in the potential that is controlled by the receptor conformation. As a result, one is led to introduce two rate constants for the receptor/ligand bond dissociation,

$$k_1(f) = k_1^0 \exp\left(\frac{x_1 f}{T}\right),$$

$$k_2(f) = k_2^0 \exp\left(\frac{x_2 f}{T}\right),$$

where k_1^0 and k_2^0 are the rate constants for $f = 0$, and x_1 and x_2 are the widths of the barriers associated with each well (Fig. 2 *a*).

Note that the exponents describing the force dependence of $k_1(f)$ and $k_2(f)$ above have the same sign, in contrast to the rate constants for the transitions between the two states of the allosteric site (Eq. 3). The bond dissociation rate constants of the two-pathway model (Eq. 1) also have different signs. In contrast to the two-pathway model (12), bond dissociation in the allosteric model (19,45) occurs via a single pathway.

As the allosteric site of the receptor protein fluctuates between two conformations, the active site also fluctuates between two states. The overall rate for the bond dissociation is given by the weighted average of the rates corresponding to each state of the active state,

$$k(t,f) = k_1(f)P_1(t,f) + k_2(f)P_2(t,f), \quad (4)$$

with the weights given by the probabilities from Eqs. 2 and 3. The probability $P(t,f)$ of finding the receptor/ligand bond intact is given by

$$\frac{dP(t,f)}{dt} + k(t,f)P(t,f) = 0. \quad (5)$$

To describe the experimental data, one needs to solve Eqs. 2 and 3 to obtain $P_1(t,f)$ and $P_2(t,f)$. Then, one can solve Eq. 5 with the rate coefficient defined in Eq. 4 and obtain $P(t,f)$ as a function of t and f. Generally, it is hard to solve the problem analytically, especially if the force varies with time. The problem can be simplified significantly using the separation of the timescale for the allosteric transition and bond dissociation.

TIMESCALE SEPARATION AND TRANSFORMATION TO THE TWO-PATHWAY MODEL

Small proteins typically fold within microseconds, whereas folding of larger proteins takes milliseconds (47–49). One can expect that large-scale structural transitions in proteins occur on similar or faster timescales. In comparison, the lifetimes of receptor/ligand bonds in the systems under consideration are much longer, ranging from fractions of seconds to several seconds. Further, in experiments with time-dependent forces, the force changes on the timescale of 0.01–0.1 s. Therefore, it is reasonable to assume that allosteric transitions are much faster than dissociation of the receptor/ligand bond, and that on the timescale of the experiment, the allosteric subsystem always remains in thermodynamic equilibrium.

This assumption eliminates the need to solve Eqs. 2 and 3 explicitly, because the experimental timescale corresponds to the long-time limit of these equations, and the solution at long times is given by the equilibrium probabilities (10) that are obtained by setting the left-hand-sides of the expressions in Eq. 3 to zero,

$$P_1(f) = \frac{1}{1 + \beta \exp\left[\frac{x_d f}{T}\right]}, P_2(f) = 1 - P_1(f), \quad (6)$$

where $\beta = k_{12}^0/k_{21}^0$ is the ratio of the rate constants for the forward and backward transitions between the two states of the allosteric site, and $x_d + x_{12} + x_{21}$. The probabilities in Eq. 6 vary with time only if the force itself is time-dependent.

The simplified model given by Eqs. 4–6 contains six independent parameters, instead of the eight parameters in the original model as represented by Eqs. 2–5. To map the allosteric model onto the two-pathway model, the problem should be simplified further, because the two-pathway model contains only four parameters (12).

Recent experiments with FimH/mannose and P-selectin/PSGL-1 have shown (43,44) that upon ligand binding (the first step, refer to Fig. 1), the distribution of conformations of the receptor protein changes to significantly increase the population of the extended state, i.e., state $a2$ in Fig. 2 *a*. This implies that the ratio of the rate constants describing transitions between states $a1$ and $a2$ of the allosteric site is $\beta = k_{12}^0/k_{21}^0 >> 1$. Hence, approximately, $P_1(f) \approx \beta^{-1} \exp[-x_d f/T]$ and $P_2(f) \approx 1$. Taking this into account allows us to express the rate constant for the receptor/ligand bond dissociation from Eq. 4 as

$$k(f) \approx k_1^0 \beta^{-1} \exp\left[\frac{-(x_d - x_1)f}{T}\right] + k_2^0 \exp\left[\frac{x_2 f}{T}\right]. \quad (7)$$

By redefining the parameters of the above expression,

$$k_s^0 = k_2^0,\ x_s = x_2,\ k_c^0 = k_1^0 \beta^{-1}, \text{ and } x_c = x_d - x_1, \quad (8)$$

we obtain the two-pathway expression for the bond dissociate rate constant (Eq. 1). To achieve the catch-behavior it is essential that $x_d > x_1$, such that $x_c > 0$. Thus, the separation of the timescales of the allosteric transition and bond dissociation, together with the assumption that the allosteric fragment of the receptor protein in the bound receptor/ligand complex exists primarily in state $a2$ (the extended state), reduce the full allosteric model to the two-pathway model (12).

The mapping of the allosteric model onto the two-pathway model gives an explicit meaning to the catch-dissociation pathway. Namely, the catch-regime of bond dissociation is related to the transition of the allosteric site from the extended ($a2$) to the bent ($a1$) conformation,

followed by escape of the ligand from the shallower state $l2$ (see Fig. 2 *a*). The parameters of the catch pathway barrier (k_c^0, x_c) depend on the properties of both active (k_1^0, x_1) and allosteric ($\beta = k_{12}^0/k_{21}^0$, $x_d = x_{12} + x_{21}$) sites.

The mapping between the two-pathway and allosteric descriptions leads to the following physical picture of the catch-binding phenomenon (see Figs. 1 and 2): The receptor protein contains an allosteric fragment involving two protein domains. In thermodynamic equilibrium, the two-domain fragment fluctuates between the bent and extended states. The bent state is more stable in the free receptor. However, ligand binding shifts the equilibrium between the bent and extended states of the allosteric fragment toward the extended state (44), because the extended state facilitates much stronger receptor/ligand binding compared to the bent state (Fig. 2 *a*). Nevertheless, in the absence of force, the receptor/ligand bond dissociates primarily by making a transition to the bent state of the allosteric fragment, which provides a much weaker receptor/ligand binding. This allosteric mechanism of bond dissociation corresponds to the catch pathway in the two-pathway model (Fig. 2 *b*). The applied force prevents the transition of the allosteric fragment into the bent state, keeping it extended. In the extended state, the receptor/ligand bond dissociates via the typical slip mechanism.

THE P-SELECTIN/PSGL-1 COMPLEX

In this and the following sections we will apply the formal results obtained above to the two best studied catch-bond systems (2,3,10,50). Both constant force and jump/ramp experimental scenarios will be considered. It should be noted that the experimental ramp rates are significantly smaller than the rates of transitions between the two states of the allosteric fragment. Therefore, the equilibrium assumption for the allosteric site can be applied to both constant force and jump/ramp scenarios. In addition to fitting the experimental data we will test the validity of the approximations taken in mapping the allosteric model (19) of catch-binding onto the two-pathway model (12).

Constant force experiments

P-selectin is an allosteric protein (see Springer (43) and references therein). The connection between the allosteric and two-pathway models given by Eq. 8, together with the earlier analysis of the P-selectin/PSGL-1 system performed within the limits of the two-pathway model (12), allows us to analyze the system using the allosteric interpretation. The analysis of the experimental lifetime

$$\tau(f) = \frac{1}{k(f)} \tag{9}$$

of the P-selectin/PSGL-1 bond subjected to a constant force has led to the following values of the parameters for the two-pathway model: $k_s^0 = 0.25\ s^{-1}$, $x_s = 5.1$ Å, $k_c^0 = 120\ s^{-1}$, and $x_c = 21.7$ Å (12).

As shown above in Eq. 8, the slip-pathway of the two-pathway model (Fig. 2 *b*) corresponds directly to the bond dissociation pathway from state 2 of the active site of the allosteric model (Fig. 2 *a*). Hence, the parameters for state 2 are $k_2^0 = 0.25\ s^{-1}$ and $x_2 = 5.1$ Å. Assuming that the allosteric transition changes only the strength of the receptor/ligand interaction, i.e., the well-depth, but not the width of the free energy barrier, we obtain $x_1 = x_2 = 5.1$ Å. Then, the relationship $x_c = x_d - x_1$ leads to the following value for the distance between the two minima in the free energy profile for the allosteric site: $x_d = 26.8$ Å. This value indicates that the allosteric transition involves significantly larger distances than bond dissociation, as expected.

The dissociation rate constant k_c^0 for the catch-pathway of the two-pathway model corresponds to a combination of the two parameters, k_1^0, β, of the allosteric model, seen in Eq. 8. To establish both parameters, we need to consider the more general version of the allosteric description, from Eqs. 4–6, which treats k_1^0 and β independently. Using Eqs. 4–6 to fit the experimental data (12), we obtain $\beta = 25.1$. Indeed, $\beta >> 1$, confirming that the reduction of the allosteric model to the two-pathway model is valid for the P-selectin/PSGL-1 complex. Given β and k_c^0, we determine $k_1^0 = 3012\ s^{-1}$.

The interpretation of the catch-binding phenomenon that follows from the allosteric model, together with the values of the model parameters for the P-selectin/PSGL-1 system established above, lead us to the following biophysical rationalization of the catch-slip dependence of the bond lifetime: In the absence of force, the allosteric site exists in the extended state $a2$ with high probability, $P_2 \approx 0.96$ (derived with Eq. 6). The lower-energy, extended state of the allosteric fragment of the receptor protein generates a deep minimum for the binding site, which exists in state $l2$ with the same high probability, $P_2 \approx 0.96$. The dissociation rate of the ligand in state $l2$ is small, $k_2^0 = 0.25\ s^{-1}$. In contrast, the probability for the ligand to be in state $l1$ of the active site is small, $P_1 \approx 0.04$. However, state $l1$ is shallow, and the ligand dissociation rate for this state is high, $k_1^0 = 3012\ s^{-1}$. Because of the high dissociation rate, the ligand leaves the binding pocket primarily with the route involving state $l1$ corresponding to the bent conformation $a1$ of the receptor protein, even though the population of state $l1$ is small. In particular, according to Eqs. 4 and 7, $k_1^0 P_1 \approx 120.5\ s^{-1}$, whereas $k_2^0 P_2 \approx 0.24\ s^{-1}$.

In the presence of the external force, the rate coefficient for the ligand dissociation from well $l1$ grows exponentially with force, $\sim\exp(x_1,f)$. At the same time the probability $P_1(f)$ to find the ligand is state $l1$ decreases exponentially also, $\sim\exp(-x_d,f)$ (see Eq. 6). Because the dimension x_d associated with the conformational change in the allosteric site is significantly larger than the change x_1 in the

receptor/ligand bond length needed to reach the barrier top, the overall rate coefficient for the bond dissociation changes with applied force as $k_1(f)P_1(f) \sim \exp(-x_d f)$, according to Eqs. 4 and 7. Hence, the bond lifetime increases, resulting in the catch behavior. The lifetime growth will continue as long as the ligand dissociates primarily via well $l1$. At a certain value of the force, the second term in Eqs. 4 and 7 will become larger than the first term, and the ligand will start dissociating via the channel associated with well $l2$. At this point, the probability for the ligand to exist in state $l2$ will be close to unity, and the bond-dissociation rate-coefficient will grow exponentially according to the second term in Eq. 7. Such switch between the two dissociation channels associated with the two conformations of the receptor protein in the allosteric model creates a one-to-one correspondence with the transition between the two pathways in the two-pathway model.

Fig. 3 shows the force dependence of the bond lifetime, represented in Eq. 9, for the P-selectin/PSGL-1 complex in the constant force experiments. The experimental data are taken from Marshall et al. (2) in the representation used in Pereverzev et al. (12). The theoretical curve represents two separate calculations of $k(f)$, using the more general formulation of the allosteric model from Eqs. 4 and 6, in addition to the mapping between the allosteric and two-pathway descriptions given by Eqs. 7 and 8. The two theoretical results coincide, because $\beta >> 1$, and Eqs. 7 and 8 provide an excellent approximation to Eqs. 4 and 6.

Fig. 4 shows the force dependence of the probability $P_1(f)$for the allosteric site to exist in state $a1$ (see Fig. 2 *a*). The black-solid line corresponds to P-selectin/PSGL-1, while the red-dashed line describes FimH/mannose. In both cases the probability is small initially and decreases further with increasing force. It is this decrease of $P_1(f)$ that is responsible for the catch-behavior of the receptor/ligand bonds.

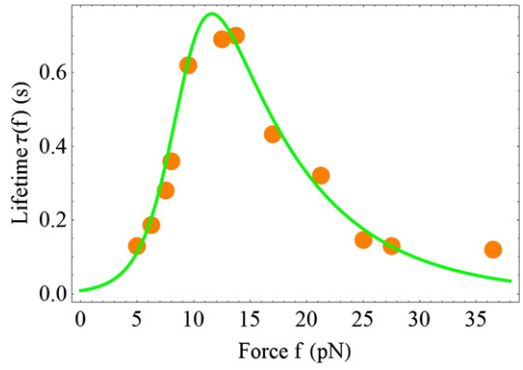

FIGURE 3 Lifetime of the P-selectin/PSGL-1 complex as a function of force in the constant force experiments. (*Dots*) Experimental data (2). (*Curve*) Theoretical results for the allosteric and two-pathway models, Eqs. 4, 5, and 6 and Eq. 1, respectively, with the parameters presented in the text.

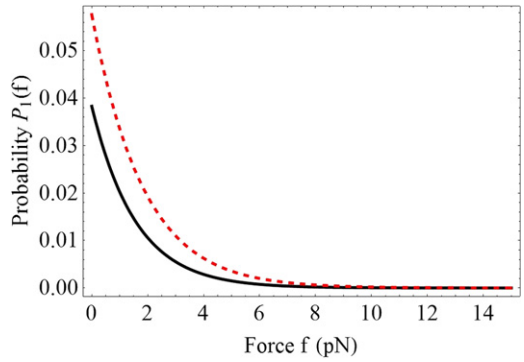

FIGURE 4 Dependence of the probability $P_1(f)$ (see Eq. 6) to find the allosteric fragment in the bent state $a1$ (see Fig 2 *b*) as a function of force for P-selectin/PSGL-1 (*solid line*) and FimH/mannose (*dashes*). Ligand binding favors the extended state (44), defining the initial value $P_1(0)$. The applied force stabilizes the extended state further. The small values of $P_1(f)$ justify the approximation leading to Eq. 7.

Jump/ramp experiments

Next, consider the mapping of the allosteric model onto the two-pathway model for the case of the applied force that grows linearly with time, as in the jump/ramp experiments (10) (r is the ramp-rate):

$$f(t) = rt. \tag{10}$$

If relaxation of the allosteric site occurs much faster than bond dissociation and the receptor protein in the receptor/ligand complex exists primarily in the extended conformation, i.e., $\beta >> 1$, then the parameters of the two-pathway and allosteric models are related by Eq. 8. According to the two-pathway model applied to the jump/ramp regime (22), the probability density of the rupture force is given by

$$p(f) = \frac{k(f)}{r}\exp\left[-\frac{k_B T}{r}g(f)\right], \tag{11}$$

where

$$g(f) = \varphi(f) - \varphi(0)$$

and

$$\varphi(f) = \frac{k_s^0}{x_s}\exp\left(\frac{x_s f}{T}\right) - \frac{k_c^0}{x_c}\exp\left(\frac{-x_c f}{T}\right).$$

The parameters corresponding to the experimental data of Evans et al. (10) were determined in Pereverzev et al. (12):

$$k_s^0 = 0.34\ \mathrm{s}^{-1},\ k_c^0 = 20\ \mathrm{s}^{-1},\ x_s = 2.1\ \text{Å},\ \text{and}\ x_c = 3.8\ \text{Å}.$$

To reconstruct parameter β, one needs to consider the allosteric model explicitly and compute $p(f)$, using Eq. 5, with the rate coefficient defined in Eq. 4 and probabilities

given in Eq. 6. The resulting expression for the rupture force probability density is more complicated,

$$p(f) = \frac{g_1(f)}{r}\exp\left\{-\frac{T}{r}[g_2(f) - g_2(0) + g_3(f) - g_3(0)]\right\}, \quad (12)$$

where

$$g_1(f) = k_1^0\frac{\exp\left(\frac{fx_1}{T}\right)}{1+\beta\exp\left(\frac{fx_d}{T}\right)} + k_2^0\beta\frac{\exp\left[\frac{f(x_1+x_d)}{T}\right]}{1+\beta\exp\left(\frac{fx_d}{T}\right)},$$

$$g_2(f) = \frac{k_1^0}{x_1}\exp\left(\frac{fx_1}{T}\right) \times Hypergeometric2F1\left[1, \frac{x_1}{x_d}, 1+\frac{x_1}{x_d}, -\beta\exp\left(\frac{fx_d}{T}\right)\right],$$

and

$$g_3(f) = \frac{k_2^0\beta}{x_1+x_d}\exp\left[\frac{f(x_1+x_d)}{T}\right] \times Hypergeometric2F1\left[1, 1+\frac{x_1}{x_d}, 2+\frac{x_1}{x_d}, -\beta\exp\left(\frac{fx_d}{T}\right)\right].$$

The orange dots in Fig. 5 show the experimental data (10) for the ramp rate $r = 1400$ pN s^{-1}. The data are presented by the ratio of the number of force rupture events measured within each of the 20-pN force intervals, to the length of the interval, i.e., as Pulls/pN. To fit the experimental data, we used the unnormalized version of Eq. 12, $p_m(f) = mp(f)$, where m is the normalization constant. The following values of the parameters were obtained: $m = 559.4$, $\beta = 131.5$, $k_1^0 = 2630$ s^{-1}, $k_2^0 = 0.34$ s^{-1}, $x_1 = x_2 = 2.1$ Å, and $x_d = 5.9$ Å. These values agree with the parameters of the two-state model (22) reported above. This is not surprising, because $\beta >> 1$. The results of both the more general version of the allosteric model, depicted in Eq. 12, and the two-pathway model, depicted in Eq. 11, are represented by the same theoretical curve in Fig. 5.

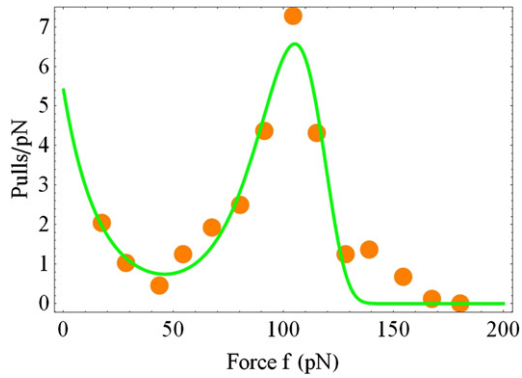

FIGURE 5 Probability density of the bond rupture force for the P-selectin/PSGL-1 complex, normalized to the total number of pulls for the ramp rate $r = 1400$ pN s^{-1}. (*Dots*) Experimental data (10). (*Curve*) Theoretical results from Eqs. 11 and 12 with the model parameters presented in the text.

The analysis of the experimental data for the P-selectin/PSGL-1 system obtained in the constant force and jump/ramp regimes indicate that the approximations taken in transforming the allosteric model into the two-pathway model are highly accurate.

THE FimH/MANNOSE COMPLEX

Constant force experiments

Le Trong et al. (44) clearly showed that FimH bound to mannose exists preferentially in the extended conformation. The angle between the lectin and pilin domains in the allosteric fragment of FimH increases upon binding, and the allosteric model (19) suggests that the allosteric site occupies state $a2$ with probability close to 1 (see Fig. 2 *a*). The extension of the allosteric fragment favors strong binding of mannose to FimH.

Similarly to the P-selectin/PSGL-1 case, we assume that there is a small probability for the allosteric site to exist in state $a1$, corresponding to the bent conformation of FimH (see Fig. 2 *a*). In this conformation, the binding of mannose to FimH is weak, and in the absence of force the bond dissociates via this pathway.

Fig. 6 shows the experimental data for the constant force experiments on the FimH/mannose complex (13,27), together with the theoretical fits using the two-pathway model from Eq. 7, and the more detailed allosteric model, seen in Eqs. 4–6. The latter description gives the following parameters: $x_1 = x_2 = 0.66$ Å, $x_d = 23.2$ Å, $k_1^0 = 179.54$ Å, $k_2^0 = 0.03$ s^{-1}, and $\beta = 16.36$. The large value of $\beta >> 1$ implies that the allosteric description of the FimH/mannose complex can be reduced to the two-pathway description seen in Eq. 1. Using Eq. 8, we obtain the following values for the parameters of the two-pathway model: $x_s = 0.66$ Å, $x_c = 22.54$ Å, $k_s^0 = 0.03$ s^{-1}, and $k_c^0 = 10.97$ s^{-1}. The

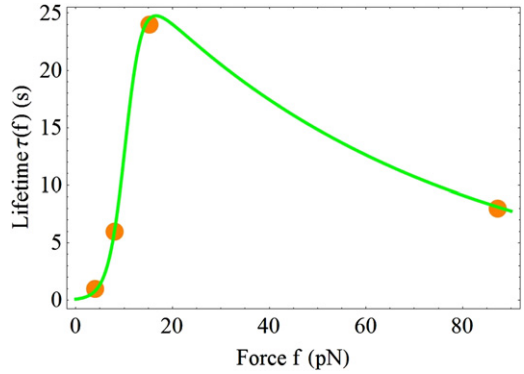

FIGURE 6 Same as Fig. 3, but for the FimH/mannose complex. The experimental data are taken from Thomas et al. (13,27).

theoretical results obtained with both models coincide on the scale of Fig. 6. They are shown by the green-solid line.

The red-dashed line presented earlier in Fig. 4 demonstrates that, indeed, the probability of finding the allosteric fragment of FimH in the bent conformation corresponding to state $a1$ in Fig. 2 a is small, and that it decreases rapidly with increasing force. At small forces, the FimH/mannose bond dissociation occurs primarily through this channel, which is responsible for catch-binding.

Jump/ramp experiments

In this section we apply the two-pathway formulation of the allosteric model to the analysis of the experimental data on the lifetime of the FimH/mannose complex subjected to the time-dependent force (51). Similarly to the P-selectin/PSGL-1 case, we will use both the more detailed allosteric model shown in Eq. 12, and using Eq. 11 that proceeds to Eq. 12 in the limit of large β. Focusing-in on the ramp rate $r = 2500$ pN/s (see Eq. 10), we will obtain the parameters of our models. The experimental data for this ramp rate were reported in Fig. 3a of Yakovenko et al. (51). The figure characterized bond rupture events that occurred within each of the 20-pN force intervals. In agreement with the data of Yakovenko et al. (51), the studies reported in Pereverzev et al. (22) showed high probability density of rupture force at small force values. The experimental data were fit with the unnormalized version of Eq. 11, $p_m(f) = mp(f)$, where m is the normalization constant.

Fig. 7 presents the experimental data (51) together with the theoretical curve corresponding to unnormalized version of Eq. 11 for the following parameter values: $m = 395.8$, $k_s^0 = 0.03\ \text{s}^{-1}$, $x_s = 2.28$ Å, $k_c^0 = 48.02\ \text{s}^{-1}$, and $x_c = 1.56$ Å. The number of pulls shown on the y-axis was divided by a factor of 20. To reconstruct the value of β, we used the more detailed allosteric model seen in Eq. 12, and the relationship between the parameters of the two models, as seen in Eq. 8. The analysis gave $\beta = 10.8$. The

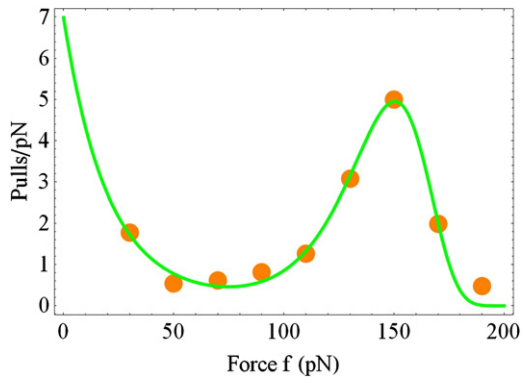

FIGURE 7 Same as Fig. 5, but for the FimH/mannose complex with the ramp-rate $r = 2500$ pN s^{-1}. The experimental data are taken from Yakovenko et al. (51).

remaining parameters are $k_1^0 = 480.2\ \text{s}^{-1}$, $k_2^0 = 0.03\ \text{s}^{-1}$, $x_1 = x_2 = 2.28$ Å, and $x_d = 3.84$ Å. Just as in the earlier examples, β is large, and the theoretical curves corresponding to Eqs. 11 and 12 coincide on the scale of Fig. 7.

The low-force region in Fig. 7 is represented only by one point, because of the difficulties in obtaining accurate experimental data at small forces. Using our models, we can estimate the contribution of the low force region into the overall bond rupture. Integration of the bond rupture probability given by Eqs. 11 and 12 over the low force region $f <$ 30 pN gives $\int_0^{30} p(f)df = 0.29$. Thus, ~30% of all bond dissociations occur at low forces corresponding to catch binding. This conclusion was obtained for the high ramp rate of $r = 2500$ pN s^{-1}. The corresponding estimate for $r = 250$ pN s^{-1}, which is 10-times slower, gives a 97% probability of bond dissociation by the catch-binding mechanism. The above result indicates that low force data are particularly important for characterization of catch-binding at small values of r. Otherwise, one can expect large errorbars in the model parameters.

ALLOSTERIC RELAXATION TIMESCALE

The results presented above were obtained under the assumption that relaxation of the allosteric fragment subjected to the external force occurs much faster than dissociation of the receptor/ligand bond. This assumption allowed us to eliminate one of the eight parameters of the full allosteric model, seen in Eqs. 2–5, and to introduce the ratio of the rate coefficients for the forward and backward transitions between the two states of the allosteric site, $\beta = k_{12}^0/k_{21}^0$. To estimate the timescale of allosteric relaxation and to evaluate the validity of this assumption, we need to consider the most detailed level of the allosteric description, as represented in Eqs. 2–5. In this section, we obtain analytic solutions of these equations for the case of constant force.

All information about the dynamics of the force-induced bond dissociation is contained in the time-dependent bond survival probability $P(t, f)$ for a given magnitude of applied force. The model presented in Eqs. 2–5 gives the second-order differential equation for the bond survival probability,

$$\frac{d^2 \ln P(t,f)}{dt^2} + \nu_a(f)\frac{d \ln P(t,f)}{dt} + \nu_a(f)\nu_l(f) = 0, \quad (13)$$

where

$$\begin{aligned} \nu_a(f) &= k_{12}(f) + k_{21}(f), \\ \nu_l(f) &= \frac{[k_1(f)k_{21}(f) + k_2(f)k_{12}(f)]}{\nu_a(f)}. \end{aligned} \quad (14)$$

The two parameters, $\nu_a(f)$ and $\nu_l(f)$, characterize the relaxation rates for the allosteric site and for the ligand in the active site. The force dependence of the rate constants

encountered in Eq. 14 has been defined above in Review of the Allosteric Model.

Solving Eq. 13 subject to the initial conditions in

$$\ln P(0,f) = 0, \left.\frac{d \ln P(t,f)}{dt}\right|_{t=0} = \nu_l(0), \qquad (15)$$

we obtain

$$\ln P(t,f) = \frac{\nu_l(f) - \nu_l(0)}{\nu_a(f)}\{\exp[-\nu_a(f)t] - 1\} - \nu_l(f)t. \qquad (16)$$

The relaxation rate $\nu_a(f)$ depends only on the parameters of the allosteric site (Eq. 14). Therefore, it characterizes this site alone. The relaxation rate $\nu_l(f)$ depends on the parameters of both allosteric and active (ligand) sites. If the relaxation of the allosteric site occurs much faster than that of the ligand site, then

$$\nu_a(f) >> \nu_l(f). \qquad (17)$$

Equation 16 reduces to $\ln P(t, f) \approx -\nu_l(f)t$, and the bond lifetime attains the simple form $\tau(f) = 1/\nu_l(f)$. This result coincides with the result derived from Eqs. 4–6 (see also Eq. 9). Further approximation, $\beta >> 1$, reduces the allosteric model to the two-pathway model (Eqs. 7 and 8).

To investigate the validity of Eq. 17, we will consider the FimH/mannose example. The parameters obtained earlier for this complex in the subsection entitled Constant Force Experiments are not sufficient for our purpose. Assuming that distances from the each minimum to the top of the barrier for the allosteric site are the same, $x_{12} = x_{21} = x_d/2$, we need to define one more parameter: e.g., k^0_{21}. Assuming that $k^0_{21} = 5\ s^{-1}$, representing a reasonable order-of-magnitude estimate, we obtain $\nu_l(0)/\nu_a(0) \approx 0.12$ for $f = 0$. As the force increases, this ratio rapidly decreases (see Fig. 8).

Analysis of the FimH/mannose complex subjected to a constant force shows that if $k^0_{21} \geq 5\ s^{-1}$, Eq. 17 holds for all forces. If $k^0_{21} < 5\ s^{-1}$, the inequality from Eq. 17 is true for all but the weakest forces, $f < 2 \div 3$ pN. If the condition in Eq. 17 is valid, $\ln P(t, f)$ drops exponentially fast to the value of $d(f) = -[\nu_l(f) - \nu_l(0)]/\nu_a(f)$. The drop happens within a very short time, on the order of $1/\nu_a(f)$. After the initial rapid exponential drop, $\ln P(t, f)$ continues to decrease linearly with time. The threshold value $d(f)$ shows anomalous force dependence. Such anomalies in the time and force dependence of the logarithm of the bond survival probability $\ln P(t, f)$ were seen in a number of experiments (5,13,51).

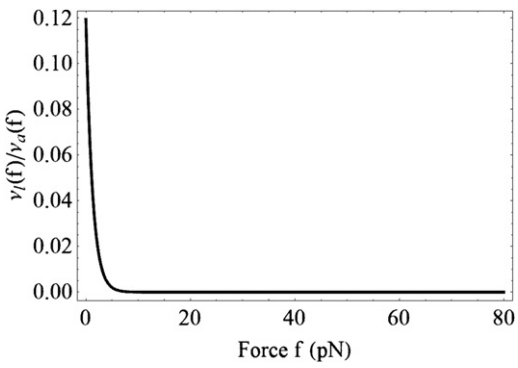

FIGURE 8 Force dependence of the ratio of the relaxation rates $\nu_l(f)/\nu_a(f)$ from Eq. 14, obtained using the model parameters for the FimH/mannose complex and $k^0_{21} = 5\ s^{-1}$.

Finally, we would like to point out that the expression for the lifetime $\tau(f) = \int_0^\infty P(t,f)dt$ in combination with Eq. 16 for $P(t, f)$ leads to

$$\tau(f) = \left\{\Gamma\left[\frac{\nu_l(f)}{\nu_a(f)}\right] - \Gamma\left[\frac{\nu_l(f)}{\nu_a(f)}, \frac{(\nu_l(f) - \nu_l(0))}{\nu_a(f)}\right]\right\} \times \frac{\exp\left[\frac{-\nu_l(0)}{\nu_a(f)}\right]}{\nu_a(f)}, \qquad (18)$$

where $\Gamma(z)$ is the Euler γ-function and $\Gamma(z,a)$ is the generalized incomplete γ-function. The curve plotted using Eq. 18 with the parameters obtained above for the FimH/mannose complex and $k^0_{21} = 5\ s^{-1}$ coincides with the theoretical curve shown in Fig. 5. This fact supports the conclusion that if $\nu_a(f) >> \nu_l(f)$, the full allosteric model given by Eqs. 2–5 simplifies to Eqs. 4–6, and that, in the limit of $\beta >> 1$, the allosteric model reduces to the two-pathway model.

DISCUSSION AND CONCLUSIONS

A number of authors have developed eight-parameter, two-state models for the description of the catch-slip anomaly observed in the lifetimes of receptor/ligand bonds (10,11,13). Such models agree with the notion of allostery (13). The model of Pereverzev et al. (19) differs from those of Evans et al. (10), Barsegov and Thirumalai (11), and Thomas et al. (13), as it explicitly identifies the governing role of the allosteric fragment in the catch-slip transition.

A multiparameter mathematical model can be given different physical interpretations. For example, the allosteric model (13) applied to the FimH/mannose complex led to two alternative rationalizations. In one case (13), the model parameters were chosen such that in the absence of force, the strongly bound state of the ligand site was more stable than the weakly bound state. With increasing force, the strongly bound state became even more stable. In the other case (51), the model was interpreted such that the strongly bound state was less stable than the weakly bound state, in the absence of force. Only at large forces did the stability of the states revert to the initial interpretation.

Within the limits of an eight-parameter model, several parameter sets can give good description of the catch-slip

transition in the FimH/mannose complex. Similar ambiguities can be expected for the P-selectin/PSGL-1 complex. Only additional structural data (43,44) have helped to choose a unique interpretation. These studies showed that in the absence of force, the strongly bound state of the ligand is more stable.

Following the guidance provided by the studies of the receptor protein structure, we were able to show that an eight-parameter allosteric model of the catch/slip transition (19) can be reduced to the simplest four-parameter two-pathway model (12). The reduction was tested with the two complexes, P-selectin/PSGL-1 and FimH/mannose, and gave good results for both constant and time-dependent forces.

The analysis of the experimental data performed within the allosteric model provides a rationalization for the observed force history dependence of the catch-bond dissociation (52). According to our model, the low population of the bent conformation of the allosteric fragment of the receptor protein plays a particularly important role in the dissociation of the receptor/ligand catch-bonds. The bent conformation is responsible for the catch dissociation mechanism. Because the ligand-binding potential corresponding to the bent conformation of the receptor is very shallow and the population of the bent conformation of the allosteric fragment is small, weak perturbations to the receptor/ligand complex may have a strong effect on the depth and population of this binding potential. Depending on the history of the applied force, the protein structure may easily change in a manner that drastically alters or even eliminates this potential well, thereby dramatically modifying the catch-behavior or removing it altogether.

The reduction of the full allosteric model to the four-parameter, two-pathway model relies on the following two approximations: 1), the relaxation of the allosteric fragment in response to the external perturbation is rapid compared to the timescale of bond dissociation, and 2), the receptor/ligand complex has the highest probability to exist in the allosteric conformation that corresponds to strong receptor/ligand binding. The less probable allosteric conformation of the receptor protein gives weaker binding. In the cases when only the first condition is satisfied, the full allosteric model reduces to a six-parameter model.

To recapitulate, the allosteric model (19) provides three levels of description of the catch-slip transition. At the simplest level, Eqs. 7 and 8 correspond directly to the two-pathway model (12), which is shown in Eq. 1, and involves only four independent parameters. This approximation captures the most important features of catch-binding, including the key anomalies observed with the bond lifetime in constant force experiments and with the rupture force probability-density in jump/ramp experiments. The intermediate six-parameter version, presented in Eqs. 4–6, is required to establish the timescale of transitions between different states of the allosteric fragment. The full eight-parameter model represented with Eqs. 2–5 is capable of describing fine features of the experimental data, such as the rapid decay of the bond rupture probability at short times.

The research was supported by National Science Foundation grant No. CHE-1050405 and National Institutes of Health grant No. R01 AI50940.

REFERENCES

1. Thomas, W. E., E. Trintchina, …, E. V. Sokurenko. 2002. Bacterial adhesion to target cells enhanced by shear force. *Cell.* 109:913–923.
2. Marshall, B. T., M. Long, …, C. Zhu. 2003. Direct observation of catch bonds involving cell-adhesion molecules. *Nature.* 423:190–193.
3. Sarangapani, K. K., T. Yago, …, C. Zhu. 2004. Low force decelerates L-selectin dissociation from P-selectin glycoprotein ligand-1 and endoglycan. *J. Biol. Chem.* 279:2291–2298.
4. Guo, B., and W. H. Guilford. 2006. Mechanics of actomyosin bonds in different nucleotide states are tuned to muscle contraction. *Proc. Natl. Acad. Sci. USA.* 103:9844–9849.
5. Kong, F., A. J. García, …, C. Zhu. 2009. Demonstration of catch bonds between an integrin and its ligand. *J. Cell Biol.* 185:1275–1284.
6. Yago, T., J. Lou, …, C. Zhu. 2008. Platelet glycoprotein Ibα forms catch bonds with human WT vWF but not with type 2B von Willebrand disease vWF. *J. Clin. Invest.* 118:3195–3207.
7. Snook, J. H., and W. H. Guilford. 2010. The effects of load on E-selectin bond rupture and bond formation. *Cell. Mol. Bioeng.* 3:128–138.
8. Dembo, M., D. C. Torney, …, D. Hammer. 1988. The reaction-limited kinetics of membrane-to-surface adhesion and detachment. *Proc. Royal Soc. (Lond) B Biol. Sci.* 234:55–83.
9. Bartolo, D., I. Derényi, and A. Ajdari. 2002. Dynamic response of adhesion complexes: beyond the single-path picture. *Phys. Rev. E.* 65:051910.
10. Evans, E., A. Leung, …, C. Zhu. 2004. Mechanical switching and coupling between two dissociation pathways in a P-selectin adhesion bond. *Proc. Natl. Acad. Sci. USA.* 101:11281–11286.
11. Barsegov, V., and D. Thirumalai. 2005. Dynamics of unbinding of cell adhesion molecules: transition from catch to slip bonds. *Proc. Natl. Acad. Sci. USA.* 102:1835–1839.
12. Pereverzev, Y. V., O. V. Prezhdo, …, W. E. Thomas. 2005. The two-pathway model for the catch-slip transition in biological adhesion. *Biophys. J.* 89:1446–1454.
13. Thomas, W., M. Forero, …, V. Vogel. 2006. Catch-bond model derived from allostery explains force-activated bacterial adhesion. *Biophys. J.* 90:753–764.
14. Zhu, C., J. Z. Lou, and R. P. McEver. 2005. Catch bonds: physical models, structural bases, biological function and rheological relevance. *Biorheology.* 42:443–462.
15. Liu, F., Z. C. Ou-Yang, and M. Iwamoto. 2006. Dynamic disorder in receptor-ligand forced dissociation experiments. *Phys. Rev. E.* 73:010901.
16. Pereverzev, Y. V., and O. V. Prezhdo. 2006. Force-induced deformations and stability of biological bonds. *Phys. Rev. E.* 73:050902.
17. Liu, F., and Z. C. Ou-Yang. 2006. Force modulating dynamic disorder: a physical model of catch-slip bond transitions in receptor-ligand forced dissociation experiments. *Phys. Rev. E.* 74:051904.
18. Beste, M. T., and D. A. Hammer. 2008. Selectin catch-slip kinetics encode shear threshold adhesive behavior of rolling leukocytes. *Proc. Natl. Acad. Sci. USA.* 105:20716–20721.
19. Pereverzev, Y. V., O. V. Prezhdo, and E. V. Sokurenko. 2009. Allosteric role of the large-scale domain opening in biological catch-binding. *Phys. Rev. E.* 79:051913.

20. Pereverzev, Y. V., O. V. Prezhdo, and E. V. Sokurenko. 2008. Anomalously increased lifetimes of biological complexes at zero force due to the protein-water interface. *J. Phys. Chem. B.* 112:11440–11445.

21. Suzuki, Y., and O. K. Dudko. 2010. Single-molecule rupture dynamics on multidimensional landscapes. *Phys. Rev. Lett.* 104:048101.

22. Pereverzev, Y. V., O. V. Prezhdo, …, E. V. Sokurenko. 2005. Distinctive features of the biological catch bond in the jump-ramp force regime predicted by the two-pathway model. *Phys. Rev. E.* 72:010903.

23. Pereverzev, Y. V., and O. V. Prezhdo. 2006. Dissociation of biological catch-bond by periodic perturbation. *Biophys. J.* 91:L19–L21.

24. Pereverzev, Y. V., and O. V. Prezhdo. 2007. Universal laws in the force-induced unraveling of biological bonds. *Phys. Rev. E.* 75:011905.

25. Prezhdo, O. V., and Y. V. Pereverzev. 2009. Theoretical aspects of the biological catch bond. *Acc. Chem. Res.* 42:693–703.

26. Bell, G. I. 1978. Models for the specific adhesion of cells to cells. *Science.* 200:618–627.

27. Thomas, W. E., V. Vogel, and E. Sokurenko. 2008. Biophysics of catch bonds. *Annu. Rev. Biophys.* 37:399–416.

28. Gunasekaran, K., B. Ma, and R. Nussinov. 2004. Is allostery an intrinsic property of all dynamic proteins? *Proteins.* 57:433–443.

29. Hilser, V. J., B. García-Moreno E, …, S. T. Whitten. 2006. A statistical thermodynamic model of the protein ensemble. *Chem. Rev.* 106:1545–1558.

30. Henzler-Wildman, K., and D. Kern. 2007. Dynamic personalities of proteins. *Nature.* 450:964–972.

31. Bahar, I., C. Chennubhotla, and D. Tobi. 2007. Intrinsic dynamics of enzymes in the unbound state and relation to allosteric regulation. *Curr. Opin. Struct. Biol.* 17:633–640.

32. Tobi, D., and I. Bahar. 2005. Structural changes involved in protein binding correlate with intrinsic motions of proteins in the unbound state. *Proc. Natl. Acad. Sci. USA.* 102:18908–18913.

33. Whitten, S. T., B. García-Moreno E, and V. J. Hilser. 2005. Local conformational fluctuations can modulate the coupling between proton binding and global structural transitions in proteins. *Proc. Natl. Acad. Sci. USA.* 102:4282–4287.

34. Ming, D., and M. E. Wall. 2005. Allostery in a coarse-grained model of protein dynamics. *Phys. Rev. Lett.* 95:198103.

35. Choi, B., G. Zocchi, …, L. Jeanne Perry. 2005. Allosteric control through mechanical tension. *Phys. Rev. Lett.* 95:078102.

36. Chodera, J. D., N. Singhal, …, W. C. Swope. 2007. Automatic discovery of metastable states for the construction of Markov models of macromolecular conformational dynamics. *J. Chem. Phys.* 126:155101.

37. Kidd, B. A., D. Baker, and W. E. Thomas. 2009. Computation of conformational coupling in allosteric proteins. *PLOS Comput. Biol.* 5:e1000484.

38. Zuckerman, D. M. 2004. Simulation of an ensemble of conformational transitions in a united-residue model of calmodulin. *J. Phys. Chem. B.* 108:5127–5137.

39. Miyashita, O., P. G. Wolynes, and J. N. Onuchic. 2005. Simple energy landscape model for the kinetics of functional transitions in proteins. *J. Phys. Chem. B.* 109:1959–1969.

40. Pereverzev, Y. V., and O. V. Prezhdo. 2009. Deformation model for thioredoxin catalysis of disulfide bond dissociation by force. *Cell. Mol. Bioeng.* 2:255–263.

41. Krishna, V., G. S. Ayton, and G. A. Voth. 2010. Role of protein interactions in defining HIV-1 viral capsid shape and stability: a coarse-grained analysis. *Biophys. J.* 98:18–26.

42. Tchesnokova, V., P. Aprikian, …, E. Sokurenko. 2008. Integrin-like allosteric properties of the catch bond-forming FimH adhesin of *Escherichia coli*. *J. Biol. Chem.* 283:7823–7833.

43. Springer, T. A. 2009. Structural basis for selectin mechanochemistry. *Proc. Natl. Acad. Sci. USA.* 106:91–96.

44. Le Trong, I., P. Aprikian, …, W. E. Thomas. 2010. Structural basis for mechanical force regulation of the adhesin FimH via finger trap-like β-sheet twisting. *Cell.* 141:645–655.

45. Pereverzev, Y. V., O. V. Prezhdo, and E. V. Sokurenko. 2010. Regulation of catch binding by allosteric transitions. *J. Phys. Chem. B.* 114:11866–11874.

46. Dudko, O. K., G. Hummer, and A. Szabo. 2008. Theory, analysis, and interpretation of single-molecule force spectroscopy experiments. *Proc. Natl. Acad. Sci. USA.* 105:15755–15760.

47. Lee, J. C., I. J. Chang, …, J. R. Winkler. 2002. The cytochrome *c* folding landscape revealed by electron-transfer kinetics. *J. Mol. Biol.* 320:159–164.

48. Yang, W. Y., and M. Gruebele. 2003. Folding at the speed limit. *Nature.* 423:193–197.

49. Klepeis, J. L., K. Lindorff-Larsen, …, D. E. Shaw. 2009. Long-time-scale molecular dynamics simulations of protein structure and function. *Curr. Opin. Struct. Biol.* 19:120–127.

50. Gunnerson, K. N., Y. V. Pereverzev, and O. V. Prezhdo. 2009. Atomistic simulation combined with analytic theory to study the response of the P-selectin/PSGL-1 complex to an external force. *J. Phys. Chem. B.* 113:2090–2100.

51. Yakovenko, O., S. Sharma, …, W. E. Thomas. 2008. FimH forms catch bonds that are enhanced by mechanical force due to allosteric regulation. *J. Biol. Chem.* 283:11596–11605.

52. Marshall, B. T., K. K. Sarangapani, …, C. Zhu. 2005. Force history dependence of receptor-ligand dissociation. *Biophys. J.* 88:1458–1466.